A Markov chain approach to modelling charge exchange processes of an ion beam in monotonically increasing or decreasing potentials

2006 J. Phys. A: Math. Gen. 39 11119

(http://iopscience.iop.org/0305-4470/39/35/012)

INSTITUTE OF PHYSICS PUBLISHING JOURNAL OF PHYSICS A: MATHEMATICAL AND GENERAL

J. Phys. A: Math. Gen. **39** (2006) 11119–11128 doi:10.1088/0305-4470/39/35/012

A Markov chain approach to modelling charge exchange processes of an ion beam in monotonically increasing or decreasing potentials

O Shrier, J Khachan and S Bosi

School of Physics, University of Sydney, 2006, Australia

Received 26 April 2006, in final form 17 July 2006
Published 11 August 2006
Online at stacks.iop.org/JPhysA/39/11119

Abstract

A Markov chain method is presented as an alternative approach to Monte Carlo simulations of charge exchange collisions by an energetic hydrogen ion beam with a cold background hydrogen gas. This method was used to determine the average energy of the resulting energetic neutrals along the path of the beam. A comparison with Monte Carlo modelling showed a good agreement but with the advantage that it required much less computing time and produced no numerical noise. In particular, the Markov chain method works well for monotonically increasing or decreasing electrostatic potentials. Finally, a good agreement is obtained with experimental results from Doppler shift spectroscopy on energetic beams from a hollow cathode discharge. In particular, the average energy of ions that undergo charge exchange reaches a plateau that can be well below the full energy that might be expected from the applied voltage bias, depending on the background gas pressure. For example, pressures of ≈20 mTorr limit the ion energy to ≈20% of the applied voltage.

PACS numbers: 34.70.+e, 02.50.Ga, 52.65.Pp, 52.80.−s, 52.40.Mj, 52.58.Qv, 52.70.Kz

1. Introduction

Charge exchange reactions are dominant in energetic glow discharges, particularly in hollow cathode [1–7] and plane cathode [8–10] hydrogen discharges operating in the units and tens of mTorr pressure range, which exhibit directional ion beams. As a result, Doppler spectroscopy has been used as a diagnostic tool to determine the ion energy distributions. In this paper, we present a semi-analytical method that enables the rapid determination of spatial ion energy distributions for such discharges. This method will be shown to be a special case of Markov Chain theory, and a comparison is presented with the results of Monte Carlo simulations. Moreover, comparisons will be made with ion energies obtained by Doppler spectroscopy measurements on a hollow cathode hydrogen glow discharge.

It has been established [1–3, 8] that the main charge exchange reactions in a hydrogen discharge are given by

$$H^+ + H_2 \rightarrow H^* + H_2^+, \tag{1}$$

$$H_2^+ + H_2 \rightarrow H^* + H + H_2^+, \tag{2}$$

$$H_3^+ + H_2 \rightarrow H^* + H_2 + H_2^+, \tag{3}$$

where H^+, H_2^+ and H_3^+ are the principle ionic species that subsequently undergo charge exchange with the H_2 background gas resulting in hydrogen neutrals, H, that may also be in an excited state, H^*. It has also been shown [11] that the resulting fast neutrals have trajectories that are in the same direction as the incident ('parent') ions. Moreover, the total energy of the resulting fragments from the reactions is approximately equal to the energy of the incident ion. Any energy lost to electronic or vibrational excitation is only a few tens of eV and is negligible compared to the keV range of energies considered here. If the parent ion is H_2^+ then each of the H fragments will have half the energy. Similarly, for H_3^+, the fragments have one-third of the parent's energy [11]. In addition, note that a cold neutral ion, H_2^+, is created with each reaction. These cold ions can subsequently accelerate in the discharges, which have monotonically increasing or decreasing potentials, and in turn can undergo a charge exchange collision. In this paper, we will model this chain of charge exchange reactions in order to determine the spatial distribution of ion energies along a hydrogen ion beam in an H_2 background gas, which is a one-dimensional problem.

Monte Carlo modelling can easily be used to model these chain reactions except it suffers from numerical noise or long computing times. The method presented here overcomes both of these limitations. We will now present our semi-analytical and intuitive approach to this modelling and finally show that it can be derived using Markov Chain theory.

2. Semi-analytical approach

We will focus on the charge exchange reaction given in equation (2) since the density of H_2^+ is greatest in hydrogen discharges operating in the units and tens of mTorr, which is our region of interest. It has been shown by Doppler spectroscopy [2, 3] that the three species have similar energies along such an ion beam and the results of the simulations will apply equally to them. After the incident ion undergoes charge exchange, it becomes an energetic neutral and will be regarded as being lost from the system. Consequently, the newly created cold ion will then move along the beam and go through the same charge exchange process. The charge exchange cross sections are greatly dependent on the incident ion energies. Since we are dealing with energies that range from 0 to the order of 10 keV, the energy distributions are heavily dependent on the spatial electrostatic potential profile and the background gas pressure.

We assume a total beam length that consists of m segments each with a length of Δx. Thus the fraction of ions, R_{ij}, that start from segment i and undergo charge exchange along the path to segment j is given by

$$R_{ij} = 1 - \exp\left(-n\Delta x \sum_{k=1}^{j} \sigma(E_{ik})\right), \tag{4}$$

where n is the number density of the background H_2 gas, and $\sigma(E_{ik})$ is the charge exchange cross section for the ion with energy E_{ik}. As a result, the probability, P_{ij}, of particles that start in segment i and undergo charge exchange in segment j is given by

$$P_{ij} = R_{i(j+1)} - R_{ij}. \tag{5}$$

Thus the matrix of probabilities of a particle starting out in segment i and undergoing charge exchange in segment j is given by

$$\mathbf{P} = \begin{pmatrix} P_{11} & P_{12} & P_{13} & \cdots & P_{1m} \\ 0 & P_{22} & P_{23} & & P_{2m} \\ 0 & 0 & P_{33} & & P_{3m} \\ \vdots & \vdots & & \ddots & \vdots \\ 0 & \cdots & & & P_{mm} \end{pmatrix}. \tag{6}$$

We can specify the initial distribution of ion positions along the beam path by the row vector

$$\mathbf{F_0} = (f_1 \quad f_2 \quad \ldots \quad f_m), \tag{7}$$

where f_i indicates the fraction of ions initially resident in segment i, and the sum of the vector components is unity. The first segment starts from the first element of this row vector. In order to keep track of the fraction of charge exchange events in each segment, we formulate a matrix,

$$\begin{pmatrix} f_1P_{11} & f_1P_{12} & f_1P_{13} & \cdots & f_1P_{1m} \\ 0 & f_2P_{22} & f_2P_{23} & & f_2P_{2m} \\ 0 & 0 & f_3P_{33} & & f_3P_{3m} \\ \vdots & \vdots & & \ddots & \vdots \\ 0 & \cdots & & & f_mP_{mm} \end{pmatrix}, \tag{8}$$

where the starting segment of the ions is indicated by the row number, and the segment where charge exchange occurs is indicated by the column number. For example, the fraction of ions that start from the beginning of segment 1 and undergo charge exchange when they reach the end of segment 3 is given by the f_1P_{13} matrix element. However, matrix $\mathbf{P}$ does not take into account the new ions created along the beam path as a result of charge exchange. So we extend the formulation of the matrix in equation (8) such that each column of the matrix is also a source of new ions that now can accelerate and undergo charge exchange in subsequent segments. This can be represented by

$$\mathbf{D} = \begin{pmatrix} f_1P_{11} & f_1P_{12} & f_1P_{13} & \cdots & f_1P_{1m} \\ 0 & (f_2+S_1)P_{22} & (f_2+S_1)P_{23} & \cdots & (f_2+S_1)P_{2m} \\ 0 & 0 & (f_3+S_2)P_{33} & \cdots & (f_3+S_2)P_{3m} \\ \vdots & \vdots & & \ddots & \vdots \\ 0 & 0 & \cdots & 0 & (f_m+S_{m-1})P_{mm} \end{pmatrix}, \tag{9}$$

where $S_i = \sum_{q=1}^{i} D_{qi}$ is the fraction of ions from charge exchange events from segment i, which have been included as contributing to charge exchange events in further segments along the beam path. That is, S_i is the sum of the elements of column i of matrix $\mathbf{D}$ given in equation (9). For example, segment 2 will contain the fraction of ions that were generated by charge exchange in segment 1 and is given by $S_1 = f_1P_{11}$. Similarly, $S_2 = f_1P_{12} + (f_2P_{22} + S_1P_{22})$, is the fraction of all the ions that resulted from charge exchange in segment 2.

Our aim is to determine the average ion energy in each segment since this is relevant to Doppler spectroscopy measurements. Consequently, we define a matrix that contains all the possible energies of the ions in each segment, given by

$$\mathbf{E} = \begin{pmatrix} E_{11} & E_{12} & E_{13} & \cdots & E_{1m} \\ 0 & E_{22} & E_{23} & & E_{2m} \\ 0 & 0 & E_{33} & & E_{3m} \\ \vdots & & & \ddots & \vdots \\ 0 & 0 & \cdots & 0 & E_{mm} \end{pmatrix}, \tag{10}$$

where E_{ij} represents the energy of ions that started out at the beginning of segment i and have undergone charge exchange in segment j. Again, the columns of this matrix represent the segment number, and the row numbers represent the starting segment of the ions. Recall that the elements in a column of matrix **D** give the fraction of ions that have undergone charge exchange in the segment represented by that column, and the row number represents the starting segment of these ions. As a result, we can now write down the average energy, $\overline{E}_j$, of ions in any segment j as

$$\overline{E}_j = \frac{\sum_{i=1}^{j} E_{ij} D_{ij}}{\sum_{i=1}^{j} D_{ij}}. \tag{11}$$

We label this approach as being intuitive because it enables us to write down the average energy in this form. We will now show that this same result can also be obtained from Markov Chain theory. Note, however, that the Markov approach uses iterative matrix multiplication in contrast to the single matrix, **D**, where the recursiveness is naturally embedded in the S_i elements.

2.1. Markov chain method

It is clear from the previous section that the number of charge exchange events in any particular segment along a beam path greatly depends on the number of charge exchange reactions in preceding segments. This is a typical example of a Markov chain, where the outcome of a particular result is dependent on previous results. Consequently, we can obtain a row vector, $\mathbf{F_1}$, which gives the fraction of ions that have undergone charge exchange only once by

$$\begin{aligned} \mathbf{F_1} &= \mathbf{F_0 P} \\ &= (f_1 \quad f_2 \quad \ldots \quad f_m) \begin{pmatrix} P_{11} & P_{12} & P_{13} & \cdots & P_{1m} \\ 0 & P_{22} & P_{23} & \cdots & P_{2m} \\ 0 & 0 & P_{33} & \cdots & P_{3m} \\ \vdots & \vdots & & \ddots & \vdots \\ 0 & \cdots & & & P_{mm} \end{pmatrix}, \end{aligned} \tag{12}$$

where P_{ij} are the same probabilities defined in equation (5). Again, the element number in the row vector, $\mathbf{F_1}$, indicates the segment number. However, we must also include multiple charge exchange events due to low-energy ions, which subsequently accelerate and repeat the process. We take this into account by moving to the next segment and consider that to be the new starting segment thus resulting in the new probability matrix. To do this we

make use of

$$\mathbf{T} = \begin{pmatrix} 0 & 1 & 0 & \cdots & 0 \\ 0 & 0 & 1 & \cdots & 0 \\ \vdots & & & \ddots & \vdots \\ 0 & & \cdots & 0 & 1 \\ 0 & & \cdots & 0 & 0 \end{pmatrix}, \tag{13}$$

which has the property of shifting the rows of a matrix upwards, such that

$$\mathbf{TP} = \begin{pmatrix} 0 & P_{22} & P_{23} & \cdots & P_{2m} \\ 0 & 0 & P_{33} & \cdots & P_{3m} \\ \vdots & & & \ddots & \vdots \\ 0 & & \cdots & 0 & P_{mm} \\ 0 & & \cdots & 0 & 0 \end{pmatrix}. \tag{14}$$

The fraction of particles, $\mathbf{F}_N$, in any particular segment as a result of N charge exchange generations can now be written as

$$\mathbf{F}_N = \mathbf{F}_0\mathbf{P}(\mathbf{TP})^{N-1}. \tag{15}$$

As a result, we can write down a row vector,

$$\mathbf{F} = \sum_{N=1}^{m} \mathbf{F}_N, \tag{16}$$

where each segment contains the fraction of charge exchange events that have resulted from ions from any number of possible charge exchange events preceding it, and m is the total number of segments. Note that the elements of $\mathbf{F}$, which we will label as F_i, are the sum of the columns of matrix $\mathbf{D}$ given in equation (9), that is,

$$F_i = S_i = \sum_{q=1}^{i} D_{qi}. \tag{17}$$

The Markov chain method has reproduced the same result as our initial intuitive approach. However, we are also interested in determining the average energy of ions that have undergone charge exchange in each of the segments. The row vector, $\overline{\mathbf{E}}$, that contains the average energy in each segment can then be obtained by rewriting equations (15) and (16) as

$$\overline{\mathbf{E}} = \frac{\sum_{N=1}^{m} \mathbf{F}_N \bullet \mathbf{T}^{N-1}\mathbf{E}}{F_i}, \tag{18}$$

where i is again the element number of the resulting row vector of the numerator, the dot, $\bullet$, represents the Hadamard product of two matrices, i.e. the multiplication of the elements of one matrix with the corresponding elements of the other. Note that even though $\mathbf{F}_N$ represented a vector in equation (15), it must not be evaluated first in equation (18). Explicitly, this becomes

$$\overline{\mathbf{E}} = \frac{\mathbf{F_0} \sum_{N=1}^{m} \mathbf{P}(\mathbf{TP})^{N-1} \bullet \mathbf{T}^{N-1}\mathbf{E}}{F_i}. \tag{19}$$

Also note that all matrix operations are still carried out as usual from right to left, which also includes the Hadamard product. As an example, take the case of $N = 1$, which reduces that element in equation (19) to

$$\frac{\mathbf{F_0P} \bullet \mathbf{E}}{F_i}. \tag{20}$$

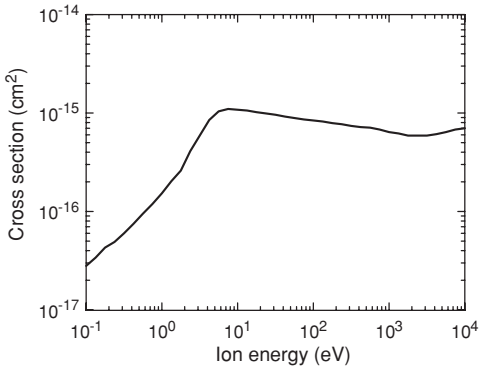

Figure 1. Charge exchange cross sections of H_2^+ with H_2 reproduced from Phelps [13].

Thus the rightmost matrix operation, which is the Hadamard product in this case, is carried out first and is given by

$$\mathbf{P} \bullet \mathbf{E} = \begin{pmatrix} P_{11}E_{11} & P_{12}E_{12} & P_{13}E_{13} & \cdots & P_{1m}E_{1m} \\ 0 & P_{22}E_{22} & P_{23}E_{23} & \cdots & P_{2m}E_{2m} \\ 0 & 0 & P_{33}E_{33} & \cdots & P_{3m}E_{3m} \\ \vdots & \vdots & & \ddots & \vdots \\ 0 & \cdots & & & P_{mm}E_{mm} \end{pmatrix}. \tag{21}$$

It is found that the average energy in each element of the vector $\overline{\mathbf{E}}$ is identical to that calculated by our earlier intuitive method given in equation (11). We will now use this approach for charge exchange modelling in a simple situation where the electric field is uniform along the beam path and compare it to Monte Carlo modelling.

3. Computational results

When we refer to the Markov chain approach in this section, we also mean the intuitive approach presented since both approaches give the same results. These methods were compared to the usual Monte Carlo method, which was carried out for a linear hydrogen ion beam accelerated in hydrogen background gas. In this approach the beam length was divided into segments and all ions were started at the beginning of the first segment. A potential difference was applied between the start and end points of the beam. As a result, the electric field across these two points was constant. Although the theory presented above can address much more complex spatial potential distributions with arbitrary ion starting positions, we explore the simplest case where ions start in the first segment since it applies to certain types of hollow cathode glow discharges that produce hydrogen ion beams. Moreover, the main acceleration region can be approximated to a constant electric field. Again, we focus on the reaction given in equation (2) since H_2^+ is the most abundant species in these discharges [2, 12].

The basic procedure for the Monte Carlo modelling was to accelerate the ions starting from the first segment, one at a time. The ion energy was calculated from the change in potential, which enabled the charge exchange cross sections to be determined from tables given by Phelps [13] and have been reproduced in figure 1. The charge exchange

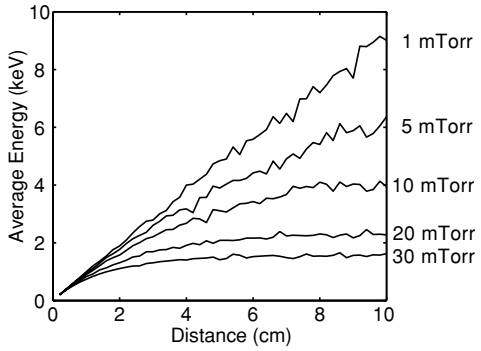

Figure 2. Monte Carlo simulations for an $H_2^+ + H_2$ charge exchange interaction in a linear potential. The average energy is given as a function of distance from an anode at a voltage of 10 kV across a 10 cm distance of beam length with operating pressures of 1, 5, 10, 20, 30 mTorr, as indicated in the figure.

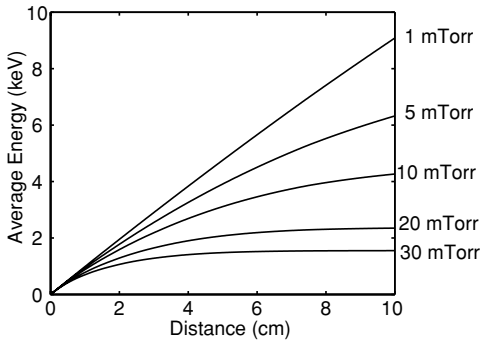

Figure 3. Average ion energy versus distance from the anode using the Markov chain approach for the same conditions as in figure 2.

probability, P, was then determined from

$$P = 1 - \exp(-n\sigma\Delta x), \tag{22}$$

where n is the number density of the background gas, σ is the charge exchange cross section and Δx is the length of a segment. A random number is then generated and if it falls within this probability, then charge exchange is considered to have taken place. As a result, the energy of the resulting neutral is stored for that segment, and a new ion is started from rest at that position. This ion is again followed along the remainder of the beam and the whole process is repeated until the end of the beam length is reached. This process is repeated for another ion starting from the first segment. With increasing number of ions, a tally is obtained of the average energy of ions that have undergone charge exchange in each segment. This enabled a comparison to be made with $\overline{E}_j$ given in equation (11).

The results of Monte Carlo modelling are presented in figure 2, where a beam path of 10 cm was used for background H_2 gas pressures of 1, 5, 10, 20, 30 mTorr. A voltage of 10 kV was applied across the beam path length. The same conditions were used for Markov chain modelling, presented in figure 3. Clearly the results of the two methods are identical, notwithstanding the numerical noise in the Monte Carlo results, where 10^4 ions were used. There was a stark difference in computational time for each of these results, where Markov chain results took in the order of seconds to complete for 100 segments, whereas the Monte

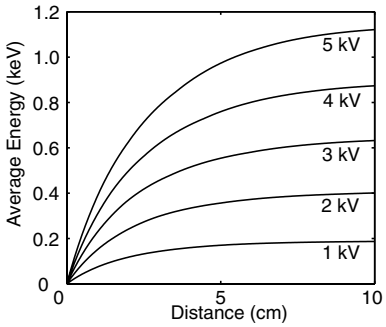

Figure 4. Average ion energy versus distance from the anode at a pressure of 20 mTorr for 1, 2, 3, 4, 5 kV across a 10 cm of beam length.

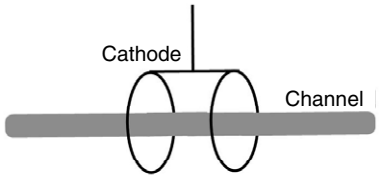

Figure 5. Double ring hollow cathode that produces a collimated and energetic discharge channel used to obtain ion energies from the cathode centre by Doppler shift spectroscopy.

Carlo approach required in the order of 10 min for 50 segments for the same microprocessor (Pentium 4) and computing language (MATLAB).

Besides computing superiority of the Markov chain approach, note that the average ion energy reaches a limiting value with increasing pressure. It is shown in figure 3 that the value of this average energy limit is at the same percentage of the applied potential for the same pressure. The results in figure 4 were obtained for a pressure of 20 mTorr and voltages ranging from 1 to 5 kV across a 10 cm length.

4. Experimental results

This approach to charge exchange modelling is suitable for discharges that produce directional ion beams in a cold background gas. In particular, there are types of hollow cathode discharges that can produce highly energetic deuterium beams such that nuclear fusion with the background gas becomes substantial [14]. Such devices consist of a mostly transparent cathode placed at the centre of a spherical anode. The resulting discharge, when operated in the units and tens of mTorr pressure range, produces discharge channels that have been shown to be highly directional [2, 3, 12].

A highly transparent cathode is presented in figure 5, which consists of two parallel stainless steel rings at the same negative potential with respect to a spherical anode wire mesh (not shown in figure 5) that surrounds this cathode. The rings were 2 cm in diameter and separated by 2 cm. This arrangement enabled a single discharge channel to be generated along the axis of the rings of the cathode. It has been shown [3, 15] from Langmuir probe measurements of the plasma potential along the axis of similar highly transparent cathodes that the spatial potential profile follows the schematic diagram given in figure 6.

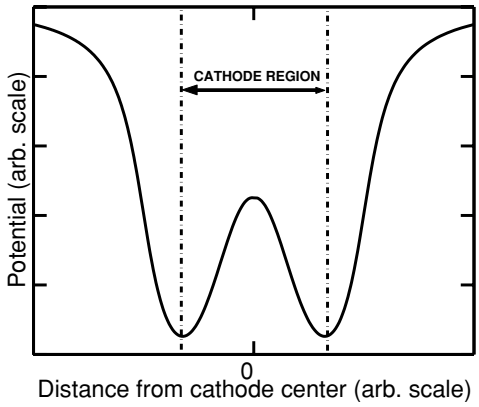

Figure 6. A schematic diagram of the electrostatic potential established in transparent hollow cathode discharges such as that shown in figure 5.

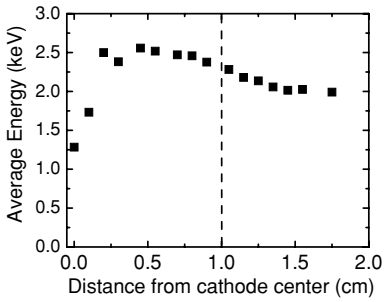

Figure 7. The spatial average energy profile of hydrogen neutrals resulting from charge exchange along the discharge channel generated by the double ring cathode. The applied cathode voltage was −10 kV at a pressure of 16 mTorr. The dashed line represents the position of the cathode ring.

Interestingly, it has been shown that, in the units and tens of mTorr pressure range, ions are generated in the cathode centre and they move outwards [1] and become energetic neutrals due to charge exchange as given by the reactions in equations (1)–(3). We can consider the region between the centre and the cathode rings (indicated by dashed vertical lines in figure 6) as having a linear potential to a first-order approximation. The Doppler spectrum of the energetic hydrogen neutrals travelling out from the centre along the discharge channel has also been measured [3] and is presented in figure 7. Note that this discharge channel represents the axis of symmetry and therefore motion along one dimension, which is the same situation that we have modelled. Consequently, the experimental results we obtained for the ion energies can be directly compared to the modelling results presented in figures 3 and 4. Clearly, from figure 7, the average energy of the excited hydrogen neutrals starts at a relatively low value from the centre and increases to a plateau at the cathode ring. The applied cathode voltage was −10 kV at a pressure of 16 mTorr. A comparison between these experimental results with the Markov chain modelling presented in figure 4 shows that there is a general agreement between them. That is, the saturation of the average energy is reached at ≈20–25% of the applied potential. The saturation effect can be qualitatively explained as a steady state that is reached between the production of cold ions that must accelerate and the disappearance of energetic ions as neutrals along the beam. This results in steady average ion energies.

However, this situation must be modelled more thoroughly since the outgoing ions that have not undergone charge exchange will be deflected back into the cathode. Moreover, ions that are created outside, by outwardly moving electrons, will also move towards the cathode. This detailed modelling will be given in a future publication.

5. Conclusions

We have developed a Markov chain approach for modelling the charge exchange process of hydrogen ion beams as an alternative to a Monte Carlo method. Moreover, an intuitive method was used but was shown to be the same as the Markov chain approach. It was found that the advantage in this approach was the rapid computing time without any numerical noise. The method was applied to hydrogen ions accelerating in a linear potential with a background H_2 gas. In addition, this was compared to Doppler shift measurements in a region of a hollow cathode discharge where the potential could be approximated as being linear. Good agreement was obtained between the experimental results and the Markov chain approach of the average energies of neutrals that have resulted from charge exchange. In particular, it was found that the average energy reaches a plateau which is well below the applied voltage bias. In this case, this limiting energy is determined by the pressure and applied voltage bias.

References

[1] Shrier O, Khachan J, Bosi S, Fitzgerald M and Evans N 2006 *Phys. Plasmas* **13** 12703
[2] Khachan J and Collis S 2001 *Phys. Plasmas* **8** 1299
[3] Khachan J, Moore D and Bosi S 2003 *Phys. Plasmas* **10** 596
[4] Benesch W and Li E 1984 *Opt. Lett.* **9** 338
[5] Ayers E and Benesch W 1988 *Phys. Rev.* A **37** 194
[6] Šišović N M, Majstorović G Lj and Konjević N 2005 *Eur. Phys. J.* D **32** 347
[7] Konjević N, Majstorović G Lj and Šišović N M 2005 *Appl. Phys. Lett.* **86** 251502
[8] Barbeau C and Jolly J 1990 *J. Phys. D: Appl. Phys.* **23** 1168
[9] Kuraica M and Konjević N 1992 *Phys. Rev.* A **46** 4429
[10] Gemišić Adamov M R, Obradović B M, Kuraica M M and Konjević N 2003 *IEEE Trans. Plasma Sci.* **31** 444
[11] McClure G W 1965 *Phys. Rev.* **140** A769
[12] Fitzgerald M, Khachan J and Bosi S 2006 *Eur. Phys. J.* D **39** 35
[13] Phelps A V 1990 *J. Phys. Chem. Ref. Data* **19** 653
[14] Hirsch R L 1967 *J. Appl. Phys.* **38** 4522
[15] Thorson T A, Durst R D, Fonck R J and Wainwright L P 1997 *Phys. Plasmas* **4** 4